HIGH-LIFT SYSTEM DESIGN BY NUMERICAL METHODS AND WIND TUNNEL VERIFICATION

M.A. Gubanova, N.N. Bragin, E.S. Perchenkov, A.Yu. Slitinskaya
Central Aerohydrodynamic Institute (TsAGI)

Keywords: *civil plane, aerodynamics, lift, flap, slat*

Abstract

The results of experimental investigations of a civil plane wing high-lift devices and its local aerodynamics are presented. The analysis of flow has been carried out by both force measurements at different Reynolds numbers and flow visualization using mini-tufts. New design of outboard slat shape is obtained by multiregime optimization method. The experimental proof of its effectiveness is given. The proposed improvements have allowed increasing the efficiency of high-lift system and providing the required level of lift.

1 Introduction

One of the major problems to be solved during aircraft design is the development of effective high-lift system. Despite of a relatively small time share of takeoff and landing regimes, they often define constraints on wing surface area and influence the whole airplane configuration. High-lift performance can increase the economic attractiveness of aircraft in operation, namely, it can increase the takeoff and payload weights as well as expand the list of airfield usage.

Previously, the high-lift performance of transport aircraft was traditionally increased by increasing the number of its structural elements [1]. Currently, there is a steady trend toward simplification of high-lift systems and reduction of the number of elements, while maintaining overall efficiency [2-5]. Usually, trailing-edge devices are limited to single- or double-slotted Fowler flaps [6, 7]. The typical leading-edge devices are slats and Kruger flaps.

The physics of the flow around multi-element airfoils and wings is very complicated. It is characterized by the presence of separation zones, including laminar separation bubbles, interaction of confluent boundary layers and wakes of various elements. Furthermore, despite the low Mach number of the incoming flow, local supersonic zones can appear on the leading edge of a slat and main wing.

Three-dimensional (3D) flow over a wing is further complicated due to geometry features (sweep, spanwise discontinuities of slats and flaps, presence of nacelles and pylons, etc.) and cross-flow phenomena, which significantly impact the boundary layer transition, the formation of 3D confluent boundary layers, the development of spanwise flow separation, etc.

Despite the significant development of computational methods [8, 9], calculations of complete aircraft configuration — including high-lift devices, engine nacelles, and small-sized elements that affect the wing local aerodynamics — remain a challenge, and require considerable time-consuming efforts [10, 11]. Therefore, calculations of complete aircraft configurations and the corresponding aerodynamic experiments are used mainly to assess the characteristics of the final configuration, while the design procedure is based on calculations of two-dimensional or simplified 3D configurations [4,6]. Due to the aforementioned difficulties, the development of final high-lift configuration is mainly carried out experimentally and requires a large amount of testing in wind tunnels, usually under high-pressure conditions.

In the present paper the data from experimental research aimed at improving the local aerodynamics of the high-lift wing of an advanced civil airplane are reported. The results of outboard slat numerical design and testing are presented. Both the force measurement results and data of flow visualization using mini-tufts are included. The proposed modifications allowed significantly enhancing the performance of high-lift system and provide a required level of lift.

2 Description of the aerodynamic model and experimental conditions

The experimental studies of high-lift devices were performed on an advanced civil airplane model in the T-128 wind tunnel at TsAGI. The model can be tested in cruise, takeoff, and landing configurations. A view of the model in the test section of the T-128 wind tunnel is shown in Fig.1.

Fig.1 The model in landing configuration in the test section of the T-128 wind tunnel.

The model wing has a span of L=2 m, trapezoidal area of S_{tr}=0.35 m^2, sweep of $\chi_{1/4}$=26.6°, and wing mean aerodynamic chord (MAC) of b_A = 0.19 m. The leading edge of the wing is straight and the trailing edge, with zero sweep on the center wing, has a smooth curvature near the break. The fuselage of the model is cylindrically shaped and has a length of L_f=1.98 m and a diameter of D_f=0.23 m. The engine through-flow nacelles, installed on pylons under the wing, have a length of L_{nac}=0.29 m and midship area (for one nacelle) of F_{nac}=0.0136 m^2. Slats, flaps, ailerons, brake flaps, spoilers, and three pairs of flap fairings (FF) are mounted on the wing. Two-segment slats are made full span with a cut-out at the pylon/slat junction. The relative area of the slats is $\bar{S}_{slat}$=13.5%. The deflection angle of slats at takeoff is $\delta_{slat,\ in/out}$=21°/24.5° and the deflection angle at landing is $\delta_{slat,\ in/out}$=24°/28°. Two-segment single-slotted flaps have a relative area of $\bar{S}_{flap}$=22.4%. The deflection angle of flaps at takeoff is δ_{flap}=18° and the deflection angle at landing is δ_{flap} =36°. The areas are defined relative to the trapezoidal area of the wing.

To investigate the possible means to improve local aerodynamics of the high-lift wing and minimize the impact of the model structure elements on the experimental results, the following additional small-sized elements were manufactured:

- Slat brackets of improved shape (Fig. 2);
- Plugs to cover the gap between the slat and the fuselage (Fig. 3);
- Plugs to cover the gaps between the slat and the nacelle pylon (Fig. 4);
- Vortex generators (strakes) installed in various positions inboard and outboard the nacelle (Fig. 5);
- Outboard slat of optimized shape (Fig.16).

The experimental study was carried out in the Mach number range of M=0.2÷0.31 and angles of attack α=–6÷26° on the model in landing configuration with free boundary layer transition on all elements. The T-128 wind tunnel allows testing both at atmospheric and high pressure (p_0=1÷4 atm), which enables obtaining Re_{MAC} numbers in the range of Re=(0.8÷3.2)×10^6. To provide qualitative information on the flow pattern, a series of flow visualization tests using mini-tufts was carried out after the force tests.

3 Experimental study of small-sized elements for local wing aerodynamics improvement

The 3D effects associated with the existence of spanwise discontinuities in high-lift devices, presence of flap and slat brackets, vortex generators, etc., significantly affect the high-lift wing aerodynamics. The influence of specific small-sized elements on the aerodynamic

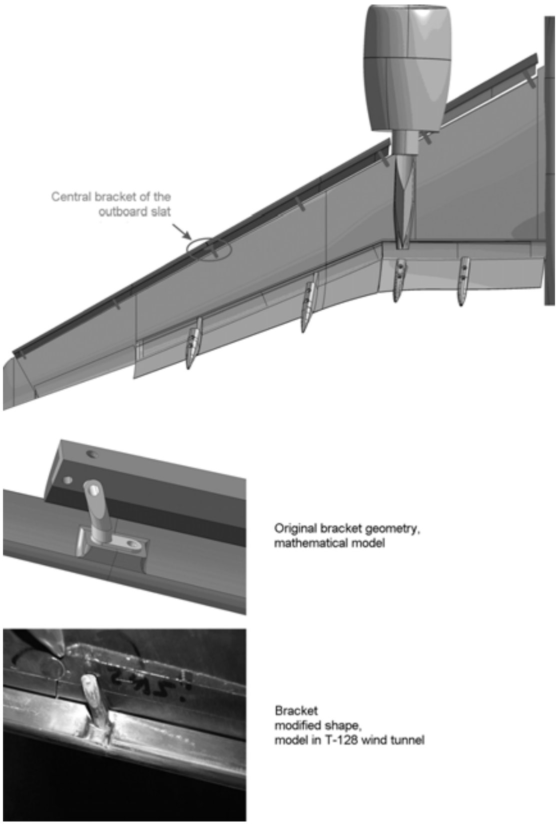

Fig. 2 Slat bracket shape modification

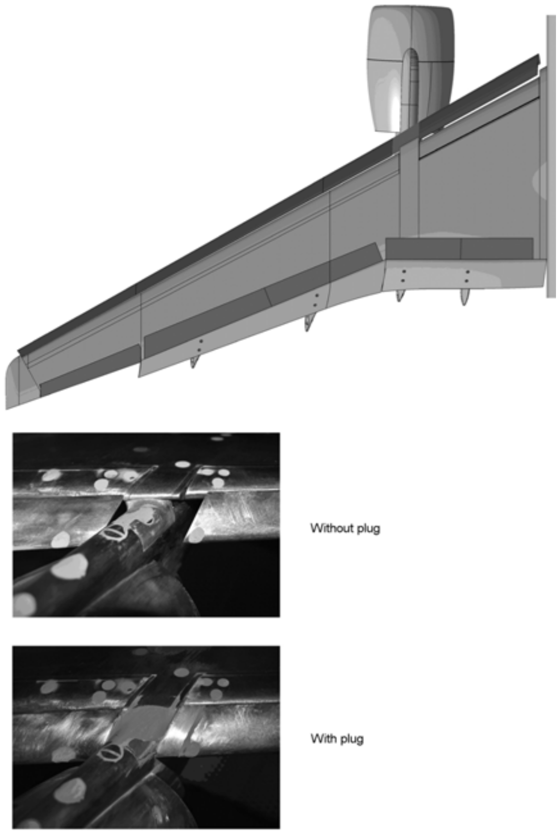

Fig. 4 Plug to cover the gaps between the slats and the nacelle pylon

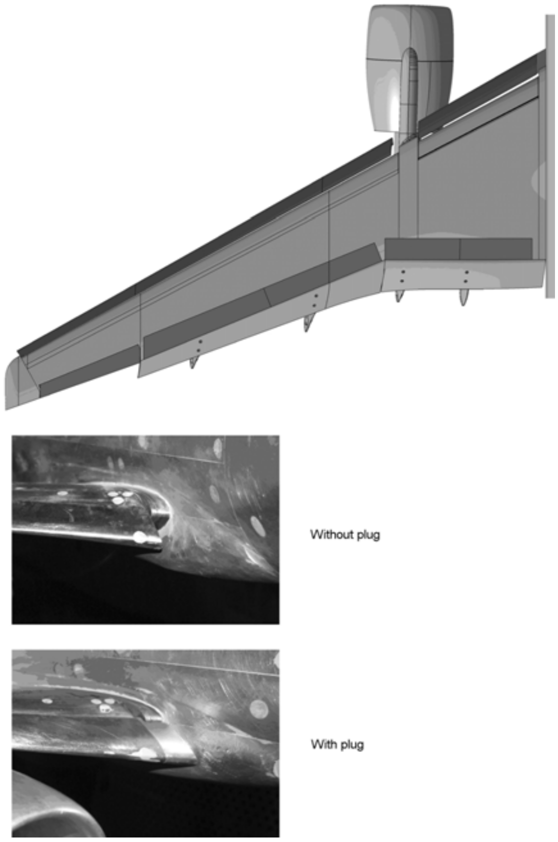

Fig. 3 Plug to cover the gap between the slat and the fuselage

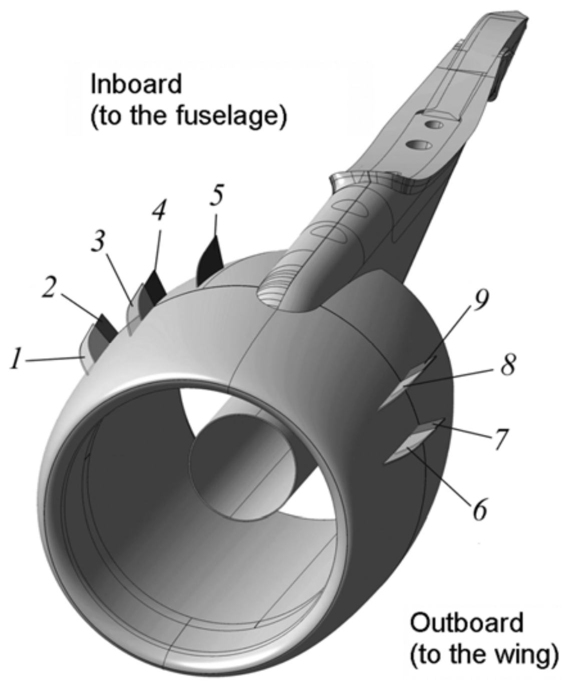

Fig. 5 Studied positions of nacelle strakes

characteristics of the model was investigated. Both the influence of individual components and the overall efficiency of various combinations of elements were studied. The modifications affected only the local geometry of the high-lift wing and did not change the shape and deflection parameters of its elements.

3.1 Study of the slat bracket shape effect

Seven slat brackets were used on each console of the model in takeoff and landing settings. The central bracket of the outboard slat, connecting two of its sections, has the most complex shape. As shown in Fig. 2, the original slat bracket was a rather massive body in the flow region between the slat and the fixed wing. Slat bracket modification consisted in a significant reduction of its volume and rounding of the outboard contours.

The results of experimental study are presented in Figs. 6 and 7, where it can be seen that a strong flow separation behind the original bracket is already developing at α=15.8°, which covers more than 20% of the wing area and limits the maximum lift of the wing. Changing the bracket shape significantly weakens the effect of overlapping the slat slot and leads to increasing the separation onset angle of attack to α≈17.5° and diminishing the separated flow area. As a result, the lift of the wing is enhanced (ΔCL_{max}=0.04 over the entire range of Reynolds numbers), and their behavior over the range of Re numbers is improved (Fig. 7). In the visualization tests, the effect of the other brackets, which have smaller dimensions, can also be seen; however, their impact on the total lift characteristics is significantly less.

All next experiments are carried out with improved slat brackets.

3.2 Search for the optimal position of strakes on the nacelle

The use of vortex generators is an effective means of improving the local aerodynamics of the wing. Vortex generators are small in size and not significantly structurally complex, but allow changing the flow around the wing considerably [12]. Nine positions of strakes, inboard (facing the fuselage) and outboard the nacelle (see Fig. 5), were examined on the model.

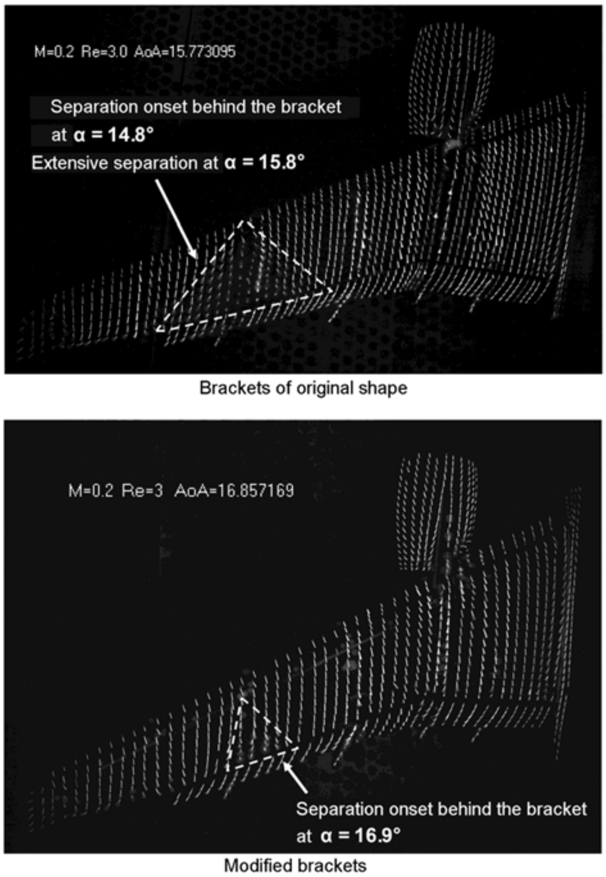

Fig. 6 Effect of the slat bracket shape on the flow above the wing

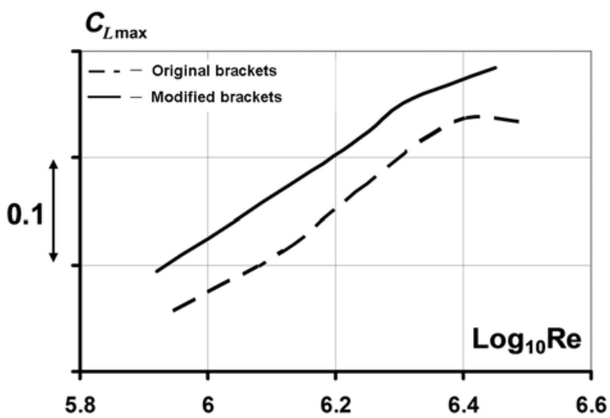

Fig. 7 Effect of the slat bracket shape on the maximum lift of the wing

The strake length was 40 mm, its height was 10 mm, and its maximum width was 1.6 mm. The positions of the strakes were determined by the coordinates of the sharpened end of vortex generator X (the distance in millimeters from the air intake along the axis of the nacelle) and δ (the angle of deviation from the nacelle symmetry plane). The following range was studied: X=0.4÷0.6L_{nac} and δ=30÷60°. The vortex generators were oriented along the calculated streamlines on the nacelle at cruise in order to minimize drag at small angles of attack. The model of the nacelle with the installed two strakes is shown in Fig. 8.

Fig. 8 Installation of vortex generators on the nacelle of the aerodynamic model

The initial search for the optimal position of the vortex generators was carried out on the model in the landing configuration at M=0.2 and low-Reynolds-number condition of $Re_{MAC}=0.8\times10^6$. The study was performed as follows: first, the best position for the inboard strake was selected; then, the installation options for the outboard strake were studied with the inboard strake set in the best position. The best positions were checked afterward at the highest $Re_{MAC}=3.2\times10^6$.

The results of experimental investigations of the optimal position of the inboard strake are presented in Figs. 9-11. Installation of a strake and formation of the corresponding vortex structures not only allow eliminating the separation on the inboard slat (Fig. 9), but also favorably affect the flow around the wing as a whole, including the delay of separation on the center wing. Based on the experimental data obtained for different positions of inboard nacelle strake, the efficiency field was identified, expressed in increments of $\Delta CL_{\max}$ (Fig. 10). The maximum efficiency at $Re_{MAC}=0.8\times10^6$ was $\Delta CL_{\max}$=0.04. The data obtained qualitatively agree with the results presented in [12]. Installation of additional vortex generators outboard the nacelle had no significant effect. Thus, the vortex generator position at the coordinates $X=0.45\cdot L_{nac}$ and δ=60° inboard the nacelle was taken as the best one. With increasing Reynolds number the beneficial effect of vortex generator installation grew about twice: at $Re_{MAC}=3\times10^6$, $\Delta CL_{\max}$=0.08 (Fig. 11).

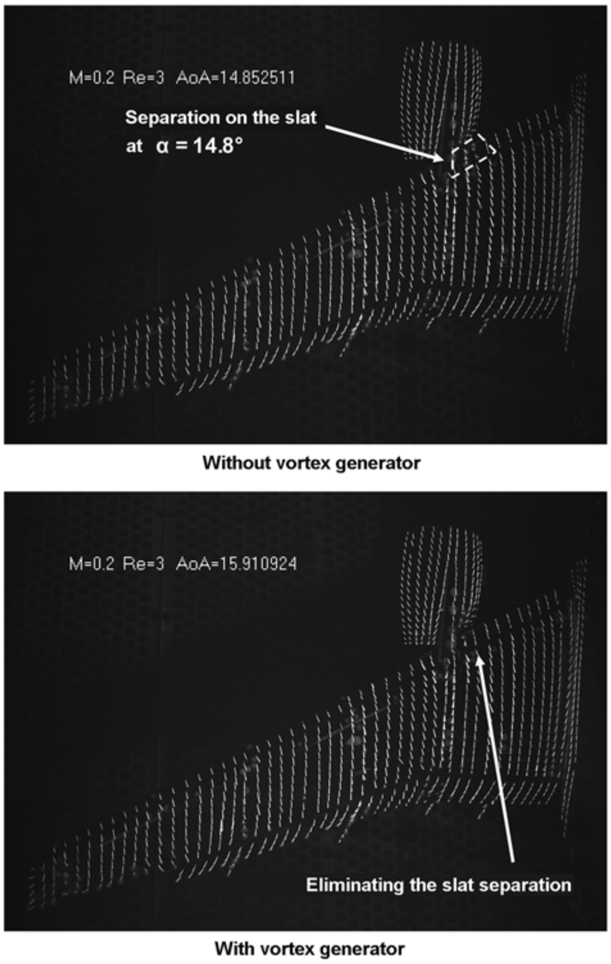

Fig. 9. Effect of the vortex generator installed inboard the nacelle on the flow above the wing

3.3 Influence of the slat spanwise cut-outs on the stall behavior

To study the effect of slat spanwise cut-outs, plugs were installed to close the gaps between the slat and the fuselage (see Fig. 3) and between the slat and the nacelle pylon (see Fig. 4). The tests of the plugs were performed with the nacelle inboard vortex generator in the optimal position.

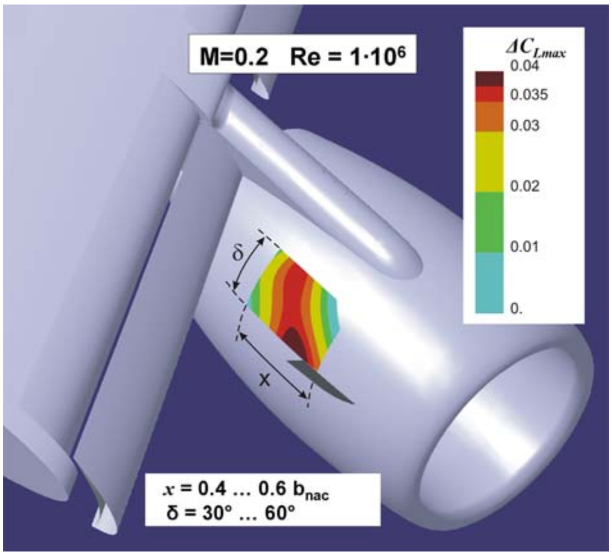

Fig. 10. Effect of the inboard vortex generator position on the maximum lift at $Re_{MAC}=1\times10^6$

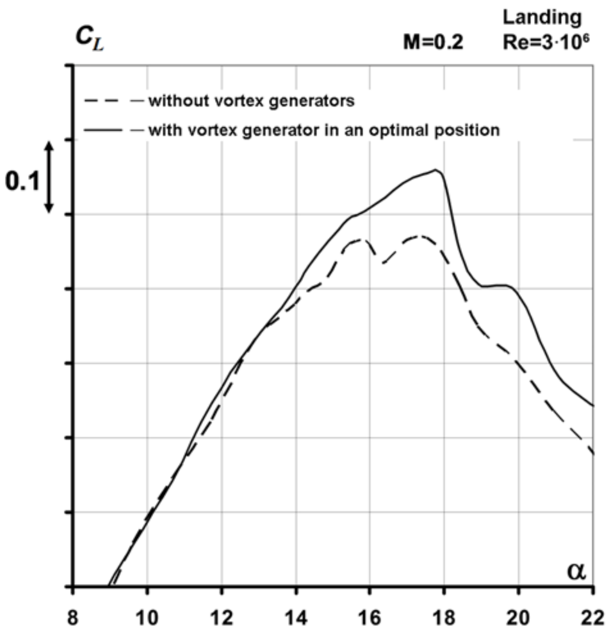

Fig. 11. Effect of the inboard nacelle vortex generator on the lift of the wing at $Re_{MAC}=3\times10^6$

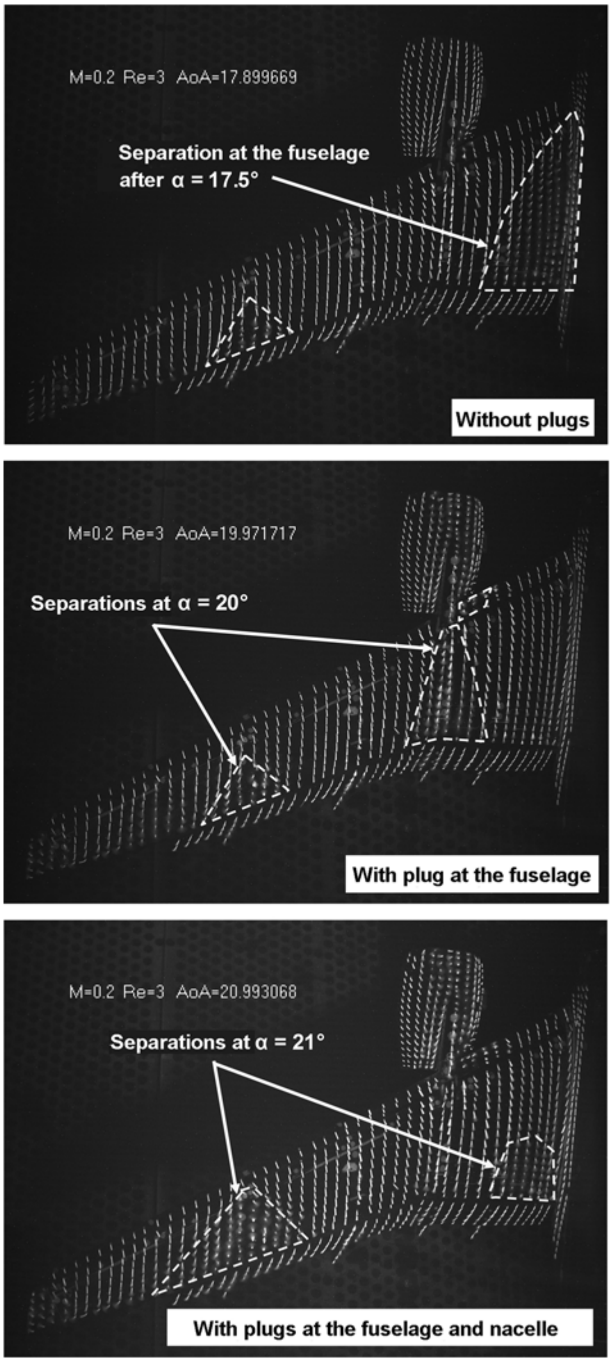

Fig. 12. Effect of the gaps in the slat on the flow above the wing

The experiments were carried out on the model in landing configuration at M=0.2 and $Re_{MAC}=3.2\times10^6$. The test results are presented in Figs. 12-14. With the presence of gaps, a strong separation above the upper wing surface exists at $\alpha=17.5°$ near the fuselage (Fig. 12). Eliminating the gap between the root slat and the fuselage shifts the development of separation up to $\alpha=20°$, with the separation being initiated behind the nacelle; the size of the separation zone is reduced, and the increase of the wing lift equals $\Delta CL_{\max,\ plug1}=0.05$, without noticeable degradation of the pitching moment behavior (Fig. 13). Similar results on the effect of the gap between the fuselage and the deflected slat on the aerodynamic characteristics are presented in [13]. The so called horn on the slat may be considered as more feasible mean to improve the local aerodynamics in this region, which may be a part of the fairing between the leading edge of the wing and the fuselage.

The size of the gaps in the slat was 10 mm outboard the nacelle pylon and 3 mm inboard (see Fig. 4). Only eliminating the gaps at the nacelle pylon itself is not so effective; improvement is obtained up to $\Delta CL_{max,\ plug2}$=0.02 (Fig. 14). Apparently, this is due to the fact that the flow in this region is already under the influence of vortices generated by the nacelle strake.

The total efficiency of two plugs, obtained experimentally, was $\Delta CL_{max,\ plug1,plug2}$=0.1 (Fig. 14). In this case, the separation is generated at the fuselage and behind the slat bracket (Fig. 12). The resulting efficiency is greater than the sum of individual efficiencies of two plugs $\Delta CL_{max,\ plug1}+\Delta CL_{max,\ plug2}$=0.07; however, this discrepancy is within the repeatability of the results of single tests in the wind tunnel near CL_{max}.

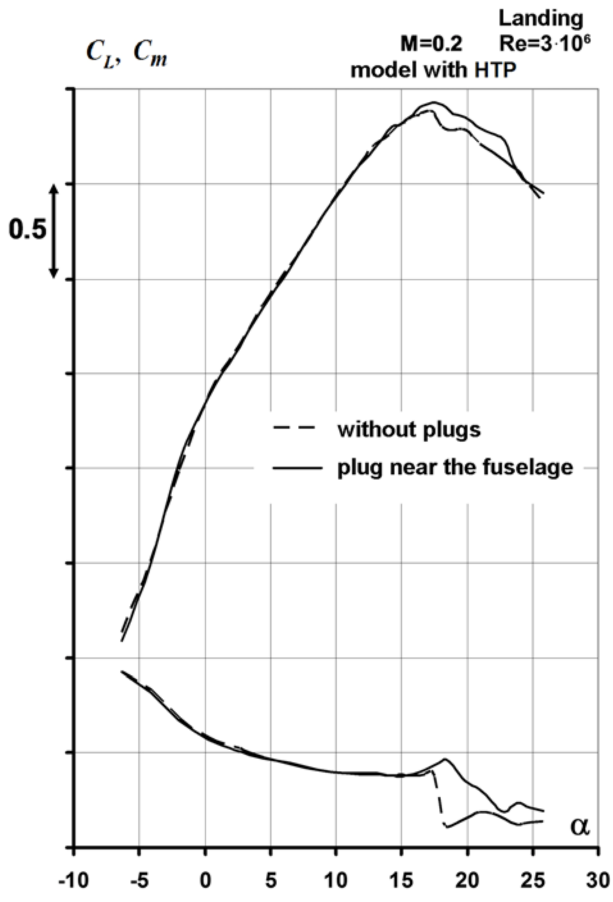

Fig. 13. Effect of the slot between the fuselage and the deflected slat on the model WT characteristics

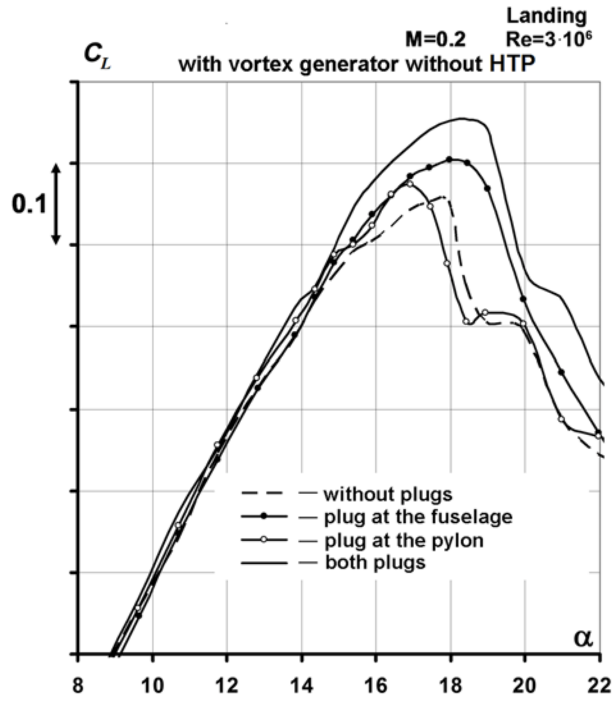

Fig. 14. Effect of the slat spanwise cut-outs on the model lift

4 Design of outboard slat by multiregime optimization method

Using the method of simultaneous multiregime optimization of wing cruise and low-speed characteristics, developed at TsAGI [14, 15], the attempt was made to enhance wing lift by redesigning outboard slat shape.

This optimization method is an efficient tool for wing aerodynamic design giving possibility to take into account both cruise and low-speed performances through the maximization of common objective function, for example,

$$Obj = w\cdot(L/D)_{mean} + (1-w)\cdot 10\cdot Cl_{max} \qquad (1)$$

where $\cdot(L/D)_{mean}$ is averaged for several cruise regimes, Cl_{max} corresponds to high-lift regime, multiplier 10 is introduced for balancing both terms and the weight factor $0<w<1$ accounts for the relative importance of cruise and high-lift efficiency.

The lift of wing without high-lift devices is considered with the assumption that additional ΔCl_{max} on isolated wing will lead to the similar increase of Cl_{max} of the wing with high-lift devices extended. As a rule, this is the case in authors' practice, if there are no any unfavorable local flow disturbances.

Experience in application of described optimization procedure and analysis of trade-off curves (Pareto-fronts) show that a significant advance in low-speed lift can be obtained at the cost of negligible losses in cruise L/D.

4.1 Slat shape numerical optimization

For slat design the optimization procedure was run with geometry variations restricted to wing leading edge (up to local slat chord length) shape variations.

For the wing without high-lift devices the increase of maximum lift of $\Delta Cl_{max}=0.05$ was obtained by cost of $\Delta(L/D)_{cruise}=-0.1$ loss (this corresponds to weight coefficient w≈0.9). In general, geometry changes can be described as some wing profiles leading edge droop and increase of the leading edge radius, Fig. 15. This correlates with general recommendations on this issue [6, 16].

Fig. 15. Example of wing section modification

Based on optimized wing shape the new outboard slats were designed (Fig. 16), then manufactured and tested on existing model.

4.2 Experimental study of optimized outboard slat

The experiments were carried out on the model in landing configuration at M=0.2 and $Re_{MAC}=3.2\times10^6$.

Fig. 17 and 18 give the comparison of test results with initial and optimized outboard slat. In first tests no advance in lift were obtained with new slat, although its effect appears as additional lift on post-stall regimes at α=18-23°, Fig. 17. The analysis of CL(α) and Cm(α) behavior and previous test results (Fig. 13-15) helped to assume that despite of console lift growing the maximum lift in both cases is restricted by strong separation above the upper wing surface near the fuselage which appears at

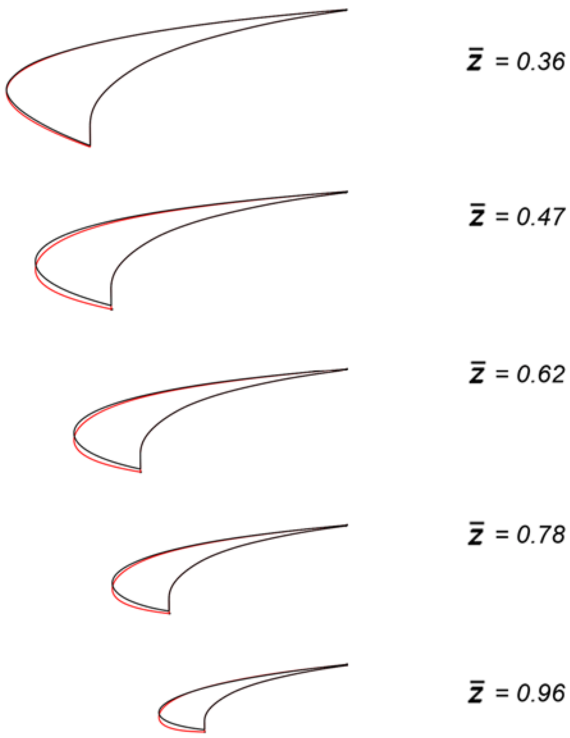

Fig. 16. Comparison of initial and optimized slat shape

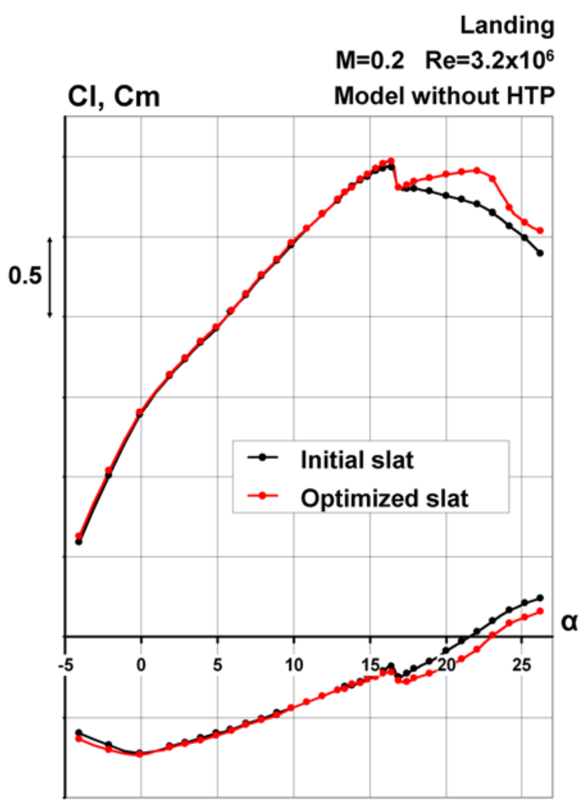

Fig.17. Effect of outboard slat shape modification with open slots

α=17°. The elimination of this separation by plug at the fuselage gives possibility to realize the advance in maximum lift provided by new slat, Fig. 18: ΔCL_{max}=0.07. For authors' pleasure, it practically corresponds to optimization result for isolated wing.

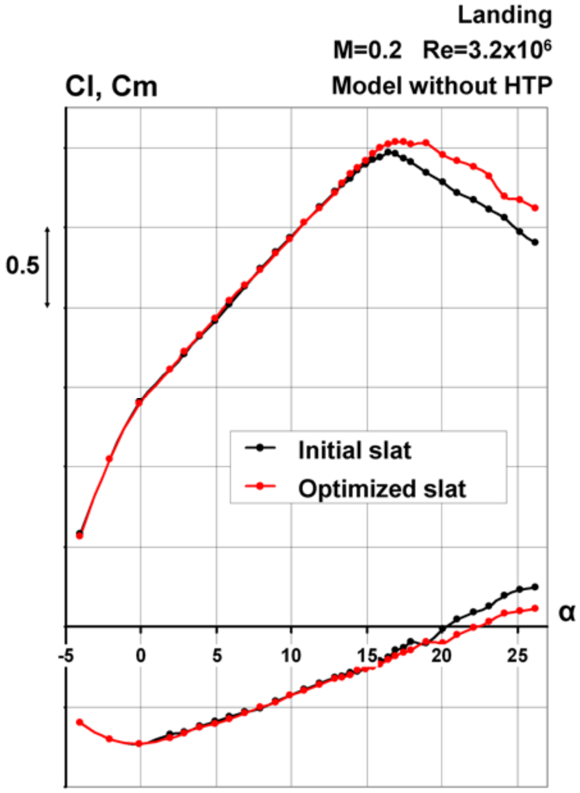

Fig. 18. Effect of outboard slat shape modification in presence of plug at the fuselage

Conclusions

The results of the experimental search of the ways to improve the local aerodynamics of high-lift wing are presented.

By application of proposed small-sized elements a total gain in maximum lift of ΔCL_{max}=0.1÷0.2 is obtained experimentally, and its Reynolds number trend is also improved (Fig. 19).

According to the presented results, the following means of improving the high-lift wing performance can be recommended as technically feasible on civil aircraft:

- Vortex generator installation inboard the nacelle;
- Minimizing the slat cut-outs at the pylon/slat junction;
- Minimizing the size of the gap between the slat and the fuselage and optimization of the slat inner end geometry.
- Redesign of particular elements without changing the construction as well as deflection angles, which can help to enhance overall wing performance.

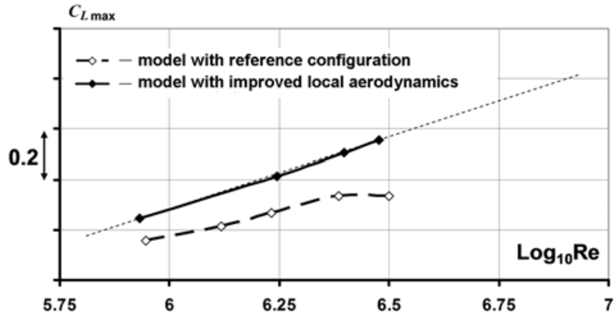

Fig. 19. Influence of the improvement of local wing aerodynamics on the overall high-lift performance

References

[1] Rudolph P K C. High-lift systems on commercial subsonic airliners, *NASA CR-4746*, 1996.

[2] Byushgens G S. Aerodynamics and Flight Dynamics of Passenger Aircraft. Moscow: Beiging, 1995 (in Russian).

[3] Rumsey C L, Ying S X. Prediction of high lift: review of present CFD capability. *Progress in Aerospace sciences*, v38 (2002), p.145-180.

[4] van Dam C P. The aerodynamic design of multi-element high-lift systems for transport airplanes. *Progress in Aerospace sciences*, v38 (2002), p.101-144.

[5] Petrov A V, Skomorokhov S I. Aerodynamics of high-lift wings, *TsAGI: Main Stages of Scientific Activity, 1993–2003*, Moscow: Fizmatlit, 2003 (in Russian).

[6] Reckzeh D. Aerodynamic design of the high-lift-wing for a Megaliner aircraft. *Aerospace Science and Technology*, №7, 2003, p107-119.

[7] Koscheev A B, Platonov A A, Khrabrov A V. *Aerodynamics of Tu-204/214 Aircraft*, Moscow: Poligon Press, 2009 (in Russian).

[8] Nikiforov V M. Calculation method for separation airfoil flow with high-lift devices at low velocities, *Uch. Zap. TsAGI*, vol. 24, no. 1, 1993 (in Russian).

[9] Wolkov A V, Lyapunov S V. Calculation method for viscous separation flow around airfoil systems, *Uch. Zap. TsAGI*, vol. 29, no. 3-4, 1998 (in Russian).

[10] Rogers S E, Roth K, Cao H V, Slotnick J P, Whitlock M, Nash S M, Baker M D. Computation of viscous flow for a Boeing-777 aircraft in landing

configuration, *Proc. Of 18th AIAA Applied Aerodynamics Conference*, AIAA Paper 2000-4221, 2000.

[11] Rudnik R. CFD assessment for high-lift flows in the European project EUROLIFT. *AIAA Paper 2003-3794*.

[12] Yokokawa Y, Kanazaki M, Murayama M, Kato H, Ito T, Yamamoto K. Investigation of the flow over nacelle/pylon and wing controlled with a vortex generator in high-lift configuration, *Proc. of 26th International Congress of the Aeronautical Sciences (ICAS)*, 2008.

[13] Kafyeke F, Pepin F, Kho C. Development of high-lift systems for the Bombardier CRJ-700, *Proc. of 23th International Congress of the Aeronautical Sciences (ICAS)*, 2002.

[14] Bolsunovsky A L, Buzoverya N P, Gubanova M A, Karas O V, Kovalev V E. Multiobjective optimization procedure for the wing aerodynamic design of the medium-haul airplane. *International Conference "Challenges in aeronautics" ASTEC'07*, August 19–22, 2007, Moscow.

[15] Gubanova M. Multiobjective optimization procedure for the wing design at cruise and low-speed conditions. *Proc. of 27th International Congress of the Aeronautical Sciences (ICAS)*, 2010.

[16] Jupp J. Wing aerodynamics and the science of compromise. *The Aeronautical Journal*, vol.105, №1053, November 2001.

mailto: skomorohov@tsagi.ru

Copyright Statement